ACS chemical biology

pubs.acs.org/acschemicalbiology

Article

Peptidic Probes to Capture Enzyme Activity Using Novel Solid Phase Compatible Warheads

Valerio Cataldi, Nikita Ostrovitsa, Fangyuan Cao, Edward W. Tate, Eoin M. Scanlan, and Joanna F. McGouran*

Cite This: https://doi.org/10.1021/acschembio.5c00771

Read Online

ACCESS | Metrics & More | Article Recommendations | Supporting Information

ABSTRACT: Activity-Based Probes (ABPs) are invaluable tools for investigating enzymatic activity but can suffer from onerous syntheses and low stability in complex proteomes. Herein, we present the first synthesis of a robust, vinyl methyl ester (VME), bearing amino acid, which is compatible with solid phase peptide synthesis (SPPS). Novel peptidic probes incorporating the VME motif were prepared, and their labeling activity was investigated against the deubiquitinating enzyme (DUB) Otubain 1 (OTUB1), a critical cysteine protease DUB with remarkable specificity for Lys48 linked polyubiquitin chains. OTUB1 is implicated in DNA repair and immune response mechanisms and is currently considered a biomarker for tumorigenesis. A probe featuring the VME warhead demonstrated high reactivity and selectivity toward OTUB1, highlighting the significant potential of this approach to create robust and selective covalent tools for interrogating cysteine isopeptidases.

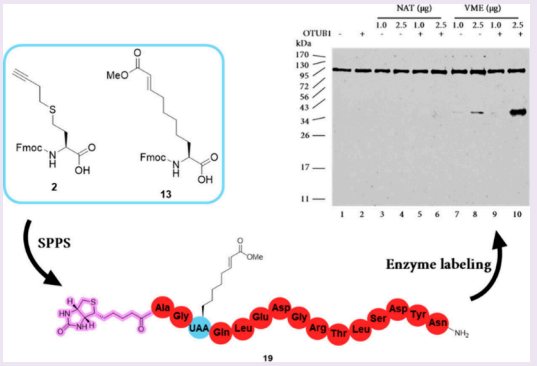

INTRODUCTION

Ubiquitination is a widespread post-translational modification (PTM) in which ubiquitin (Ub), a 76 amino acid protein, is conjugated to substrate proteins predominantly via an isopeptide bond to a lysine residue. The ATP-dependent ubiquitin conjugation machinery requires the sequential action of ubiquitin-activating enzymes (E1s), ubiquitin-conjugating enzymes (E2s), and ubiquitin-protein ligases (E3s). Depending on the structure of the target protein, additional ubiquitin moieties can be attached, resulting in multiubiquitinated substrates. Moreover, each ubiquitin contains seven different lysines (K6, K11, K27, K29, K33, K48, K63) along with an N-terminal methionine residue where the ubiquitination process can be reiterated, allowing proteins to be modified with linear or branched polyubiquitin chains.[1]

A critical characteristic of the ubiquitination machinery lies in the enzymatic reversibility of this process. Within the cell, deubiquitinating enzymes (DUBs) are responsible for disassembling or editing ubiquitin chains, further regulating ubiquitination within the cell.[2] The human genome encodes ∼100 DUBs divided into seven subfamilies, six of which are cysteine proteases. The equilibrium between ubiquitination and deubiquitination maintains cell homeostasis and controls the cellular response to stress or stimuli. Perturbations of this balance can dramatically impact cell viability, leading to disease. Dysregulation and mutation of DUBs have been linked to all the hallmarks of cancer,[3] fibrosis,[4] and autoimmune and neurodegenerative diseases.[5]

Otubain 1 (OTUB1) is an ∼35 kDa deubiquitinating enzyme of the OTU subfamily. Structurally, OTUB1 can accommodate two ubiquitin moieties: one at a distal allosteric site and another at a proximal catalytic site (Figure 1A).[6] Akin to other cysteine proteases, OTUB1 bears a catalytic triad (Cys91, His265, Asp267) to specifically cleave Lys48-linked ubiquitin chains, stabilizing target proteins and preventing their proteasomal degradation (Figure 1B).[7] In addition to this canonical isopeptidase activity, OTUB1 exhibits a non-canonical, DUB-independent regulatory function by binding to ubiquitinated E2 conjugating enzymes (e.g., UBC13, UBCH5B), thereby inhibiting further ubiquitination.[8] Accumulating evidence suggests that OTUB1 plays a critical role in tumorigenesis and DNA damage response with altered expression implicated in various cancers.[9,10] Despite the increasing interest, the complete mechanistic understanding of OTUB1 remains limited, underlining the urgent need for advanced analytical tools to study this DUB.

Activity-Based Probe Profiling (ABPP) is a valuable strategy to profile enzymatic activity and assess novel functions directly in the cellular milieu. Activity-Based Probes (ABPs) are

Received: September 23, 2025
Revised: November 18, 2025
Accepted: November 26, 2025

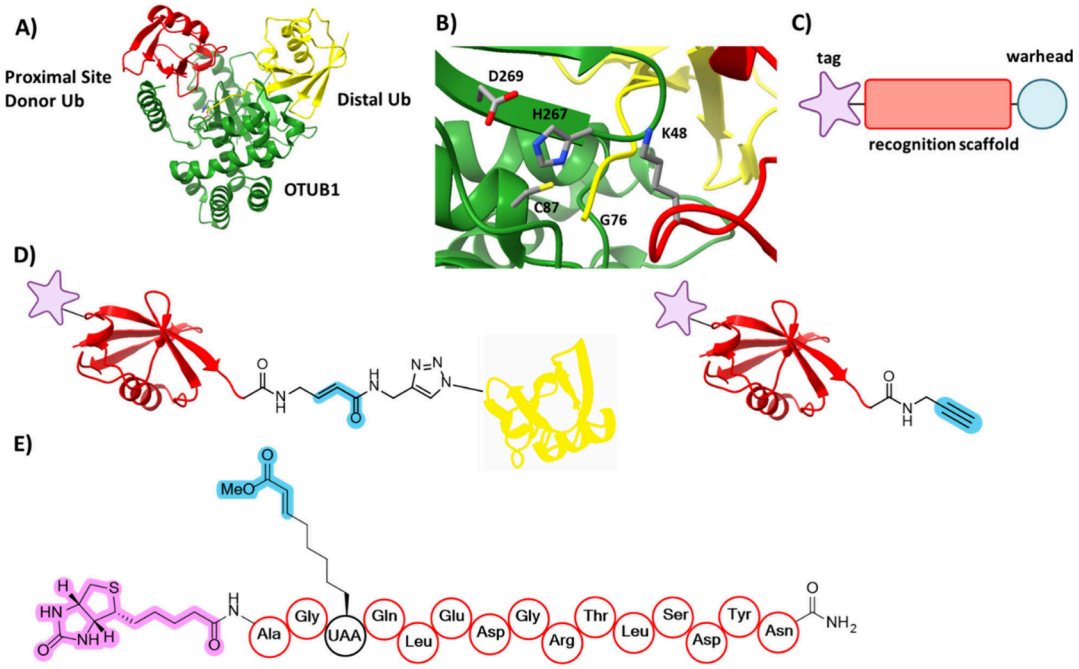

Figure 1. (A) Crystal structure of a human/worm OTUB1 (green) bound to two ubiquitin moieties (yellow in the distal site and red in the proximal site respectively; PDB structure: 4DHZ). (B) Detailed view of the active site, showing catalytic triad (Asp, His, Cys), distal Ub C-terminus (Gly76), and proximal Ub Lys 48. (C) General structure of an ABP. (D) Example of di-Ub and mono-Ub ABP used to capture DUBs. Recognition scaffold (red) consists of a recombinant ubiquitin moiety tagged at its N-terminus (purple). Semisynthetic methods are used to install the warhead (blue) at the C-terminal glycine. (E) Proposed structure for a peptide ABP. The warhead is coupled onto the recognition scaffold (red) as a UAA, and its side chain contains the electrophilic warhead (blue). Biotin is used as a tag (purple).

chemical tools that can capture the active form of an enzyme in a mechanism-based manner by covalently capturing the active site residue. ABPs are generally composed of three structural elements (Figure 1C). These include an electrophilic moiety (commonly termed the warhead), responsible for the covalent capture of the nucleophile residue in the enzyme active site. Fine tuning of the warhead determines the reactivity and selectivity of the ABP toward a specific target.[11] A recognition scaffold that confers specificity to the probe is also incorporated. Finally, a tag used for the selective capture and quantification of the ABP-enzyme covalent adduct is also included. Commonly used tags include fluorophores, biotin, or bioorthogonal groups such as terminal alkynes suitable to functionalize through click chemistry.[12]

ABPs for DUBs have been designed based on ubiquitin scaffolds incorporating a N-terminal tag and an electrophilic warhead in place of the C-terminal glycine residue of ubiquitin.[11] A variety of thiol-reactive electrophiles have been reported, including vinyl methyl ester (VME) and alkyne moieties.[13−16] These ABPs, mimicking the "acceptor" Ubiquitin, react with a broad variety of cysteine protease DUBs, providing information about global DUB activity (Figure 1D).[13,17,18] As focus shifted toward the development of DUB specific probes, recognition scaffolds were extended beyond the acceptor ubiquitin into ubiquitin-peptide and ubiquitin-protein chimeric structures.[19] However, the synthesis of these probes typically requires semisynthetic methods that can be inflexible and low yielding. Although full-length ubiquitin-based probes can be synthesized entirely via solid phase peptide synthesis (SPPS) this also requires late-stage modifications and additional purification steps.[20]

The present study aims to establish an alternative approach through the development of peptidic ABPs (Figure 1E). The probes described in this study were designed based on a peptide portion of the proximal Ub sequence wherein lysine 48 was modified to include an electrophilic warhead located at the isopeptide bond site. Basing the probe structure on the distal "donor" ubiquitin, which has a unique binding motif for OTUB1, allowed for a high degree of DUB selectivity with a simple peptidic scaffold. This is in contrast to the ubiquitin proximal "acceptor" mimicking probes discussed above, which are globally recognized by DUBs (Figure 1). The approach was designed to allow the synthesis of the ABPs via Solid Phase Peptide Synthesis (SPPS) using standard coupling reagents (Figure 1E). The warheads were incorporated into the side chain of Fmoc-protected Unnatural Amino Acids (UAAs) that were used as building blocks in SPPS for the peptidic recognition scaffold. Alongside an established Alkyne bearing UAA, we also synthesized a novel VME functionalized SPPS compatible UAA to offer a more reactive electrophilic moiety. A biotin tag was employed for visualization of the probe labeled proteins via Western blot. Importantly, this strategy was conceived as a modular approach to the synthesis of short peptides to be used as probes for DUBs, including OTUB1, or for other enzyme targets. Different warheads can be incorporated into active probes and their activity, compared with minimal effort. Moreover, the use of peptidic probes allowed rational substrate mimicking while avoiding the complexity and synthetic burden of producing full-length, protein-based probes.

RESULTS AND DISCUSSION

Probe Design and Synthesis. Generation of the probes began with the synthesis of the Fmoc-protected UAA **2** and **13** bearing electrophilic warheads designed to react with the catalytic cysteine residue in the active site of OTUB1. The

https://doi.org/10.1021/acschembio.5c00771
ACS Chem. Biol. XXXX, XXX, XXX−XXX

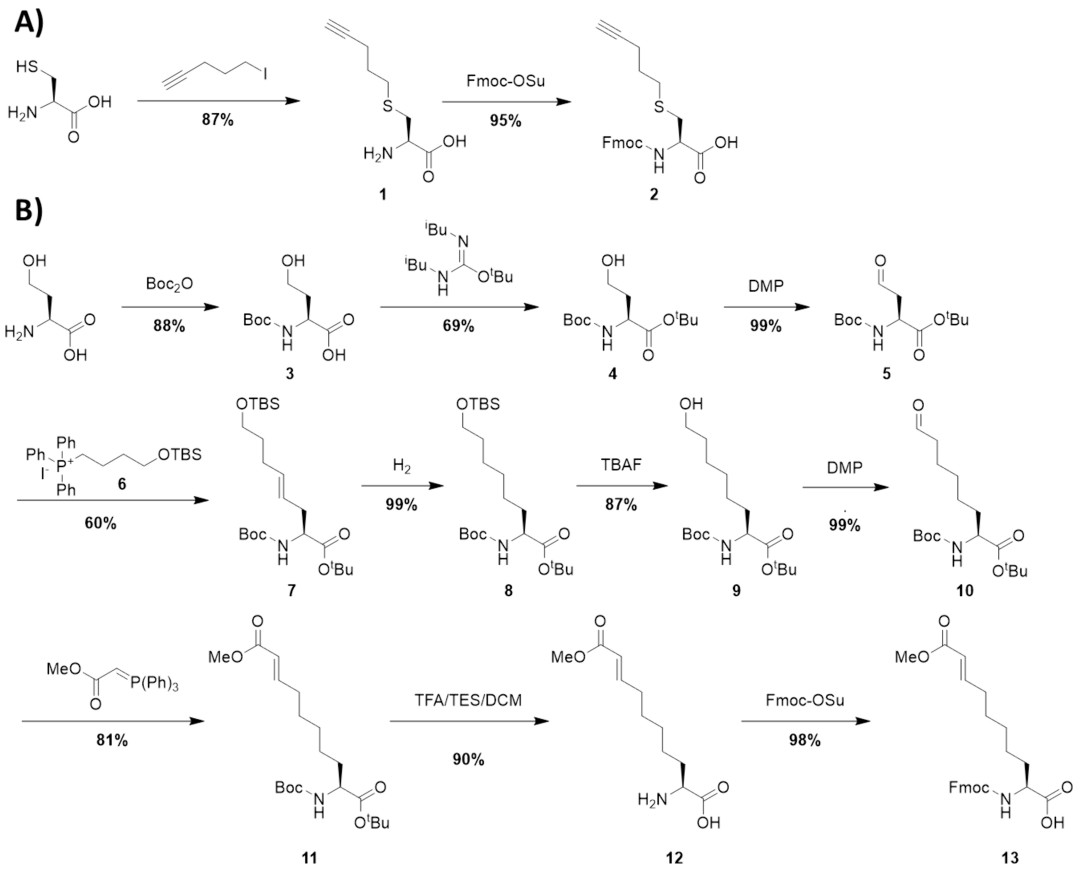

Figure 2. Synthesis of Fmoc-protected UAA **2** (A) and **13** (B).

warheads were composed of a mildly electrophilic alkyne and a more readily reactive Michael acceptor, each of which has been reported to covalently label DUBs in ABPP studies.[15,21−23]

The synthesis of alkyne bearing UAA **2** consisted of the thiol alkylation of cysteine followed by Fmoc protection (Figure 2A). The incorporation of a VME moiety into an UAA was not reported in the literature. Therefore, a 10-step synthesis was developed starting from commercially available homoserine (Figure 2B). The proposed route is operationally straightforward and requires minimal chromatographic purification, allowing the multigram preparation of a building block that is suitable for numerous SPPS coupling iterations. Homoserine was Boc protected at the N-terminus and as *tert*-butyl ester at the C-terminus, furnishing alcohol **4**, which was subsequently oxidized to the corresponding aldehyde **5** upon treatment with Dess−Martin Periodinane (DMP) in quantitative yield. The side chain of **5** was elongated using freshly prepared triphenyl phosphonium iodide **6** in a Wittig-Schlosser reaction to furnish alkene **7** in 60% yield. Hydrogenation of **7** was performed using palladium on activated carbon, which afforded **8** in quantitative yield. Subsequent deprotection of the *tert*-butyl(dimethyl)silyl (TBS) group, upon treatment with tetrabutylammonium fluoride (TBAF), yielded compound **9** in 87% yield. DMP was again used to oxidize **9** to the corresponding aldehyde **10** in an almost quantitative yield of 98%. Installation of the VME warhead on the UAA side chain was accomplished via a Wittig reaction, furnishing compound **11** in 81%. A mixture of trifluoroacetic acid (TFA) and triethylsilane (TES) was then used to simultaneously remove both the Boc and TBS protecting groups, preserving the integrity of the α,β-unsaturated methyl ester. The resulting product **12** was obtained as a TFA salt in 90% yield. In the final step, compound **12** was Fmoc-protected using Fmoc-succinimide under basic conditions to furnish the desired VME bearing amino acid target molecule **13**, which was suitable for incorporation in SPPS.

To develop a series of activity-based probes (ABPs) targeting OTUB1, we selected two peptidic Ub portions as recognition scaffolds. The first segment covers residues Gly35−Leu50, corresponding to a β-sheet region of Ub, while the second covers the less structured region Ala46−Asp60. Both peptides contain Lys48, the critical residue involved in OTUB1-catalyzed cleavage (Figure S1). The Ala46−Asp60 sequence was hypothesized to exhibit enhanced binding affinity relative to the Gly35−Leu50 sequence, owing to residues 54−60 interacting with OTUB1 through both hydrogen bonds and van der Waals interactions (Figure S2).[6] Both of the two native sequences **14** and **15** were synthesized using standard Fmoc-based SPPS, and when UAA **2** and **13** were used to replace lysine, the ABPs **16**−**19** were generated (Figure 3). Peptides **14** and **15** featuring the native lysine were designed to act as a noncovalent control, whereas the probes **16**−**19** feature reactive groups suitable for covalent labeling of the DUB OTUB1. Finally, following the final Fmoc deprotection step, the carboxylic group of biotin was coupled to the N-terminus of each peptide. On-resin biotinylation was advantageous in this approach as only a single HPLC purification step was required to obtain the fully functionalized probes with a purity greater than 90% (Figures S3−S8). With this set of probes in hand, we proceeded to test their ability to label the target enzyme OTUB1.

https://doi.org/10.1021/acschembio.5c00771
ACS Chem. Biol. XXXX, XXX, XXX−XXX

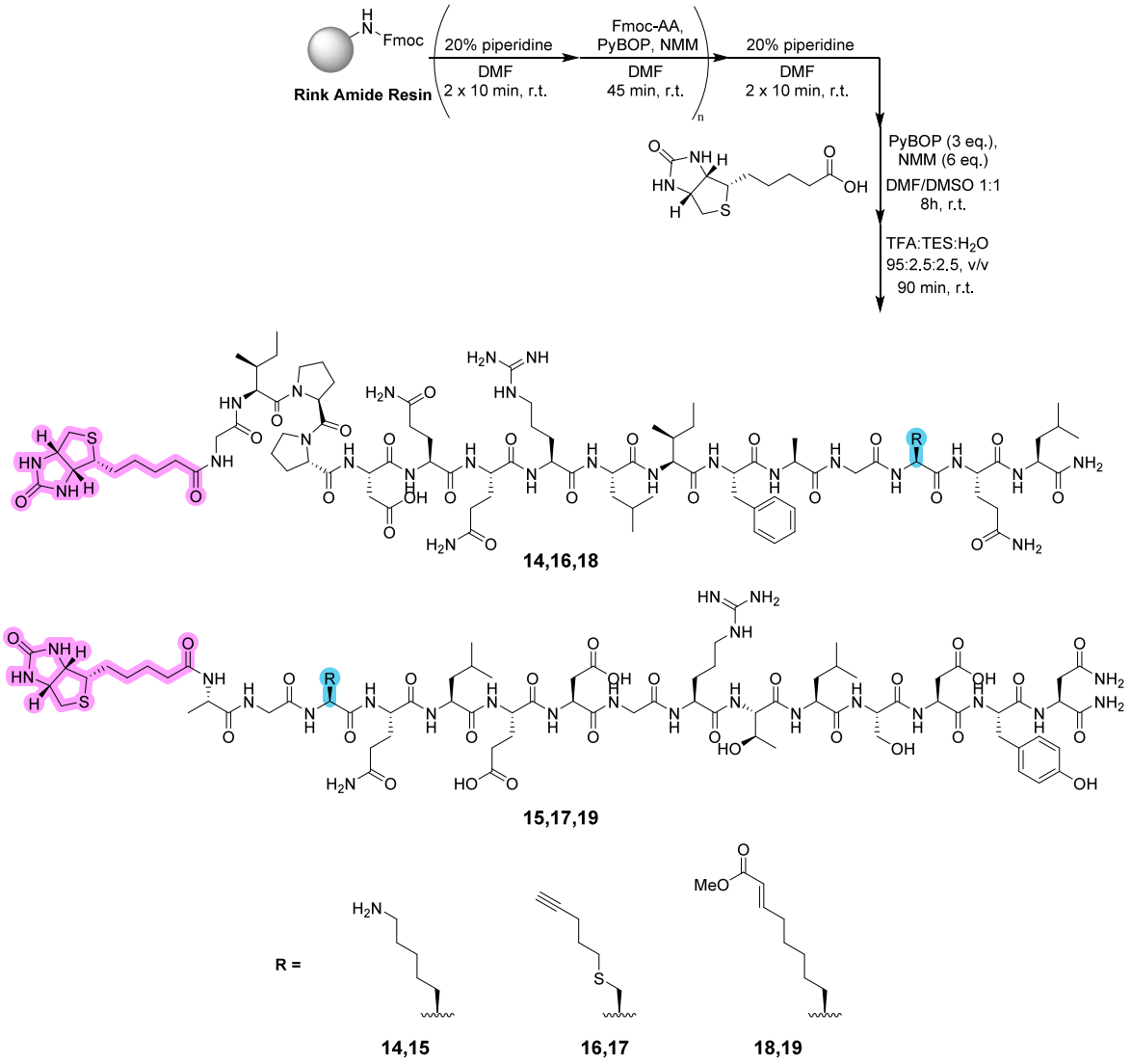

Figure 3. SPPS scheme of native biotinylated peptides **14** and **15**, along with the corresponding propargyl probes **16** and **17** and VME probes **18** and **19**. Biotin is highlighted in purple, whereas the UAA is highlighted in blue.

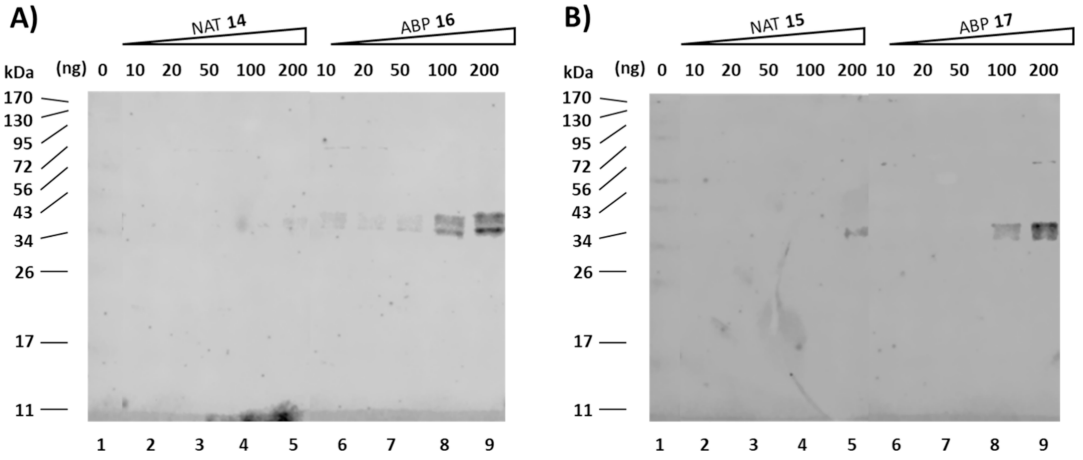

Figure 4. Antibiotin Western blot showing recombinant OTUB1 (1 μg, 0.85 μM) incubated for 1.5 h at 37 °C with increasing amounts of alkyne ABPs **16** (A, lanes **2**−**5**) from 10 ng (0.16 μM) to 200 ng (3.2 μM) and **17** (B, lanes **2**−**5**). Biotinylated native sequences **14** (A, lanes **6**−**9**) and **15** (B, lanes **6**−**9**) were used as negative controls.

Probe Evaluation. We first assessed whether the synthesized ABPs **16**−**19** were capable of labeling recombinant OTUB1. An equal amount of the enzyme was titrated against increasing amounts of alkyne probes **16** and **17** and the

https://doi.org/10.1021/acschembio.5c00771
ACS Chem. Biol. XXXX, XXX, XXX−XXX

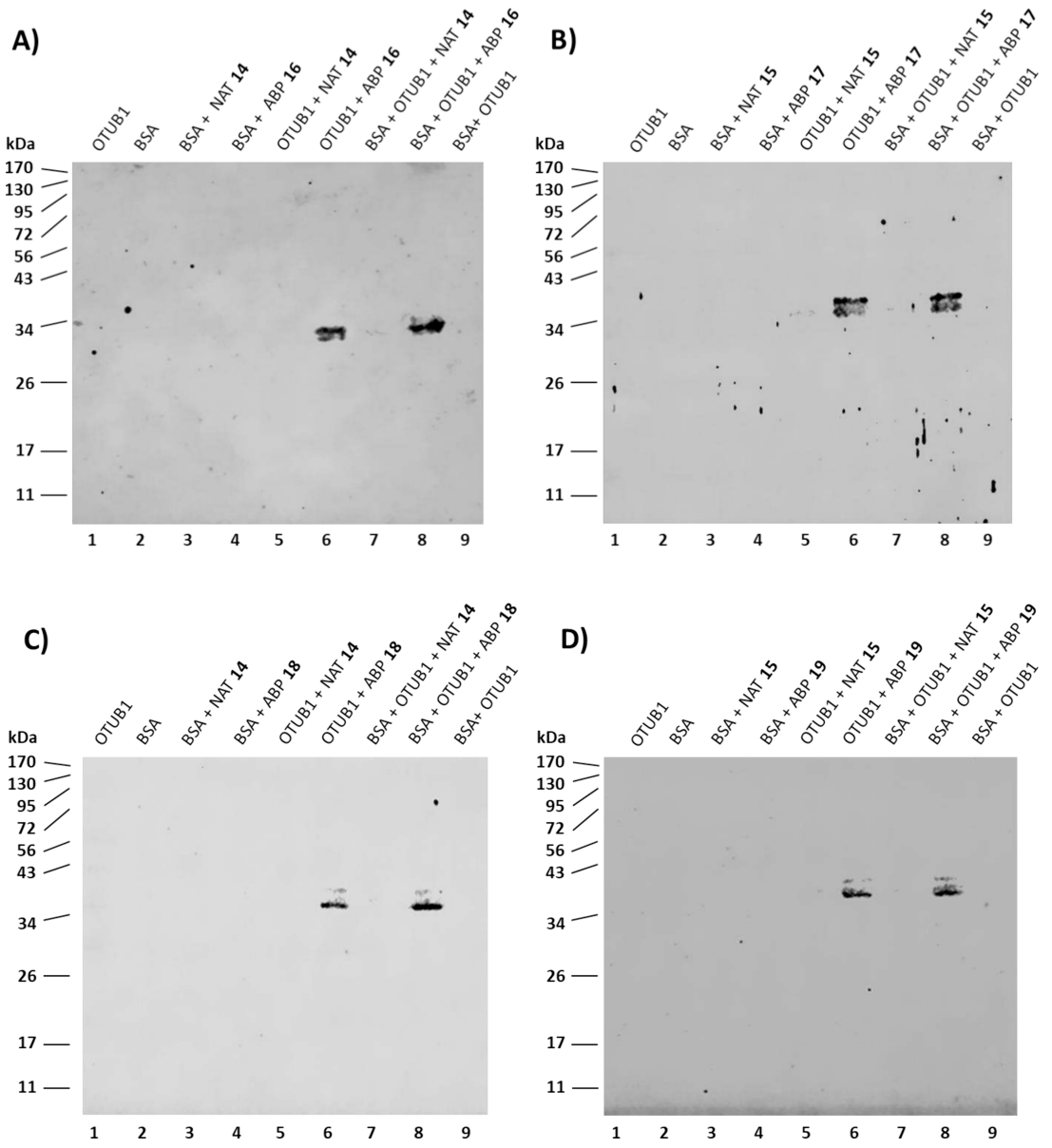

Figure 5. Antibiotin Western blot showing competition assays between recombinant OTUB1 (1 μg, 0.85 μM) and BSA (1 μg,, 0.40 μM) incubated for 1.5 h at 37 °C with 0.1 μg (1.6 μM) of (A) alkyne ABP **16** (lanes **4**, **6**, and **8**), (B) alkyne ABP **17** (lanes **4**, **6**, and **8**), (C) VME ABP **18** (lanes **4**, **6**, and **8**), and (D) VME ABP **19** (lanes **4**, **6**, and **8**). 0.1 μg (1.7 μM) of biotinylated native sequence **14** (A and C, lanes **3**, **5**, and **7**) or **15** (B and D, lanes **3**, **5**, and **7**) was used as a negative control.

corresponding native controls **14** and **15**. Following separation by gel electrophoresis, labeled OTUB1 was imaged with silver stain (Figure S9) and antibiotin Western blot (Figure 4A,B). Gratifyingly, increased labeling was observed as the probes **16** and **17** were titrated (Figure 4A,B, lanes 6−9), whereas the characteristic band around 35 kDa was not observed when OTUB1 was titrated against the native biotinylated sequences up to 100 ng, with a faint band visible at 200 ng of peptide (Figure 4A,B, lanes 2−5). The optimal results were obtained when OTUB1 was incubated with 100 ng of probes **16** and **17**, corresponding to a concentration of 1.6 μM and an ABP:OTUB1 molar ratio of 2:1 (Figure 4A,B, lanes 8). This ABP concentration was subsequently used for all the following biological assays.

We next validated the selectivity in a preliminary competition assay by incubating ABPs **16**−**17** and **18**−**19** with OTUB1 in the presence or absence of Bovine Serum Albumin (BSA), an unrelated cysteine-containing protein with a free thiol group at Cys34.[24] Following gel electrophoresis, loading of the gel was monitored by a silver stain (Figure S10), whereas labeling was followed by antibiotin Western blot (Figure 5A−D). Notably, OTUB1 was labeled by both the VME and the alkyne probes, even when coincubated with BSA (Figure 5A−D, lanes 6 and 8). As expected, no labeling for the native biotinylated sequences **14** and **15** was observed (Figure 5A−D, lanes 5 and 7). These findings suggested the peptidic ABPs were capable of selectively labeling OTUB1 even in the presence of other proteins containing reactive thiols.

To further evaluate their selectivity toward OTUB1, we tested ABPs **16**−**17** and **18**−**19** in the more complex environment of cell lysate. Human Colorectal Tumour 116 (HCT116) cell lysate was employed as it is known to express wild type OTUB1.[25] Equal amounts of HCT116 cell lysate were incubated with increasing concentrations of alkyne and

https://doi.org/10.1021/acschembio.5c00771
ACS Chem. Biol. XXXX, XXX, XXX−XXX

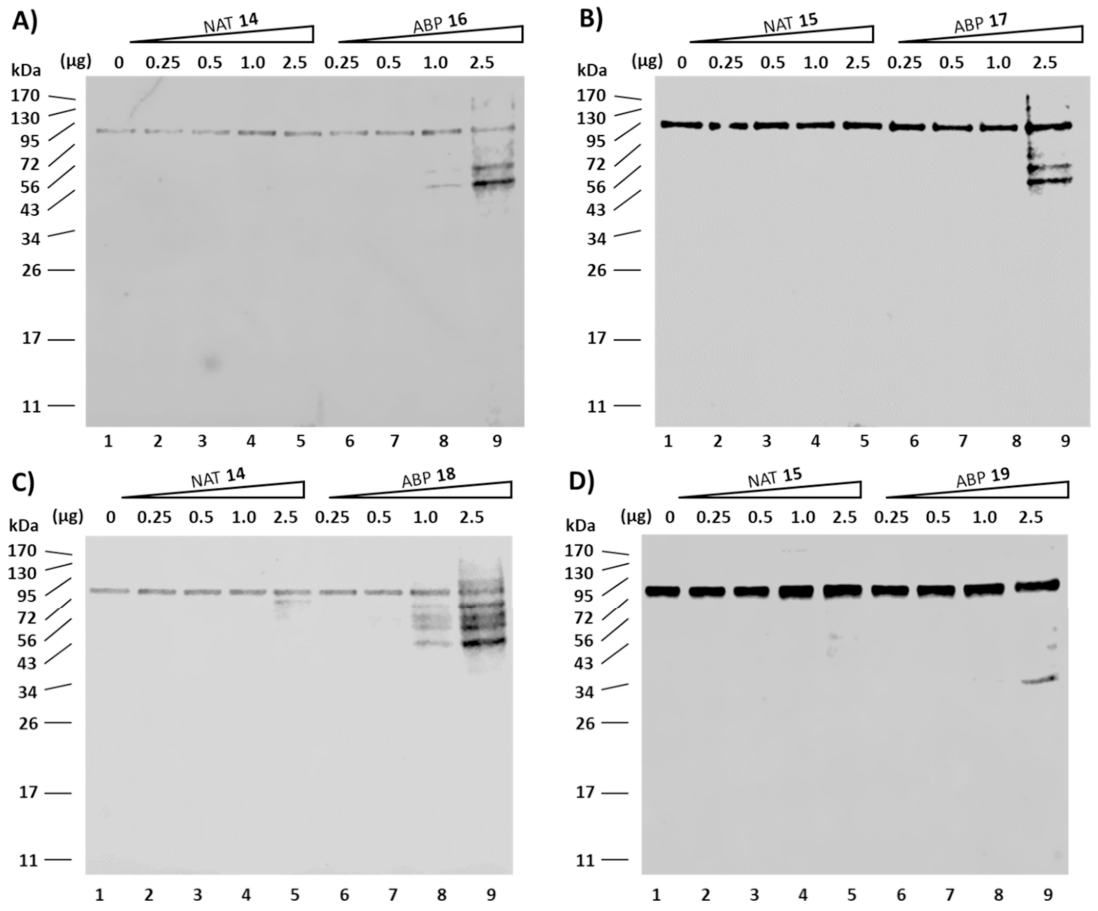

Figure 6. Antibiotin Western blot of HCT116 cell lysate (25 μg) incubated for 1 h at 37 °C with increasing quantities from 0.25 μg (4 μM) to 2.5 μg (40 μM) of (A) alkyne ABP **16** (lanes **6**–**9**), (B) alkyne ABP **17** (lanes **6**–**9**), (C) vinyl methyl ester ABP **18** (lanes **6**–**9**), and (D) vinyl methyl ester ABP **19** (lanes **6**–**9**). Native sequences **14** and **15** (A–D, lanes **2**–**5**) were used as a noncovalent control.

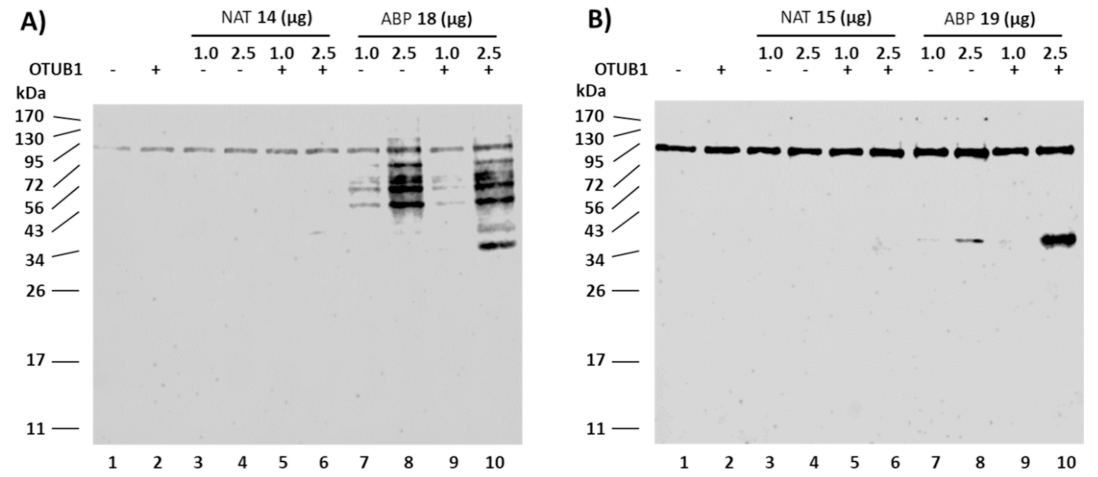

Figure 7. Antibiotin Western blot of HCT116 cell lysate (25 μg) incubated for 1 h at 37 °C with 1 μg (16 μM) or 2.5 μg (40 μM) of VME probe **18** (A, lanes 7–10) and **19** (B, lanes 7–10). Biotinylated native sequences **14** (A, lanes 3–6) and **15** (B, lanes 3–6) were used as negative controls. Recombinant OTUB1 (1 μg, 0.85 μM) was added to the cell lysate (lanes 2, 5–6, 9–10) prior to incubation.

VME ABPs **16**–**19** and control peptides **14**–**15** (Figure 6A–D). Following probe/control treatment, proteins were separated with gel electrophoresis and biotinylated species were visualized using antibiotin Western blotting. Gel loading was monitored with general silver staining (Figure S11). A consistent band around 80 kDa band was observed across all lanes, attributed to endogenous biotinylated metabolic enzymes, specifically 3-methylcrotonyl-CoA carboxylase and propionyl-CoA carboxylase.[26] As expected, control peptides **14** and **15** (lacking reactive warheads) failed to label proteins in the lysate (Figure 6A–D, lanes 2–5), confirming the necessity of the electrophilic moiety for covalent labeling. To our delight, when 2.5 μg of probes **16**–**17** and **18**–**19** was incubated with 25 μg of lysate, multiple labeled bands were

https://doi.org/10.1021/acschembio.5c00771
ACS Chem. Biol. XXXX, XXX, XXX−XXX

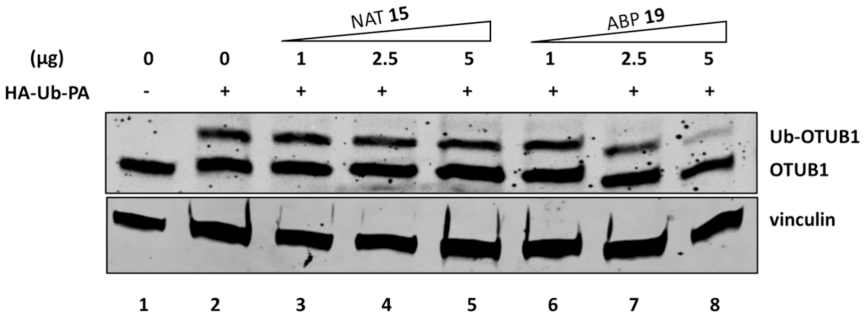

Figure 8. Western blot of HCT116 cell lysate (25 μg) incubated for 1 h at 37 °C with increasing amounts of VME probe **19** from 1 μg (16 μM) to 5 μg (78 μM) (lanes 6−8). Biotinylated native sequence **15** (lanes 3−5) was used as the negative control. Following the first incubation, the HA-Ub-PA probe (0.5 μg, 0.4 μM) was added to the cell lysate (lanes 2−8) and incubated for 45 min at 37 °C.

detected (Figure 6A−D, lane 9). Alkyne probes **16** and **17** showed similar labeling patterns but did not appear to label OTUB1, as indicated by the absence of a band at ∼35 kDa (Figure 6A,B). In contrast, VME probes **18** and **19** yielded distinct labeling profiles. Probe **18**, incorporating the VME warhead on the Gly35−Leu50 scaffold, labeled more proteins than the alkyne counterpart **16**, consistent with the higher reactivity of the VME warhead. However, it did not appear to label OTUB1 at endogenous levels in the lysate (Figure 6C). The off-target protein labeling observed in probes **16**, **17**, and **18** could be due to specific interactions such as K48 specific Ubiquitin ligases or DUBs, or they may indicate nonspecific protein labeling. Notably, probe **19**, bearing the Ala46−Asp60 scaffold and a VME warhead, successfully labeled endogenous OTUB1, as evidenced by the appearance of the expected band at 35 kDa (Figure 6D, lane 9). Moreover, the band at 35 kDa is the predominant band observed with probe **19**, showing excellent selectivity for OTUB1 at endogenous levels in the whole cell lysate.

To validate OTUB1 labeling by probes **18** and **19**, recombinant OTUB1 was spiked into the HCT116 lysate (Figures 7 and S12). In this context, probe **18** successfully labeled OTUB1 (Figure 7A, lane 10), demonstrating that its labeling efficiency improves with elevated enzyme concentration. Probe **19** confirmed its specificity by labeling OTUB1 in both native and spiked lysate samples with no other competing protein labeling observed (Figure 7B, lanes 8 and 10).

To assess whether ABP **19** could effectively label endogenous OTUB1, a competition assay between ABP **19** and HA-Ub-PA, an established DUB ABP, was performed (Figures 8 and S13). Incubation of ABP **19** with the HCT116 cell lysate was followed by a second incubation with the HA-Ub-PA probe. The HA-Ub-PA probe bears a propargylamide (PA) warhead that labels DUBs such as OTUB1 with a HA-Ub moiety, causing an ∼10 kDa mass increase on labeling by the HA-Ub-PA probe, which can be clearly seen in an anti-OTUB1 Western blot (Figure 8). To our delight, the intensity of the Ub-OTUB1 band diminished drastically upon incubation with increasing concentrations of ABP **19**. At the highest concentration of ABP **19**, the level of OTUB1 labeling with the HA-Ub-PA probe decreased >2-fold (Figure S14). The data demonstrate that ABP **19** effectively competes with HA-Ub-PA for binding of active OTUB1 within cell lysate and can block HA-Ub-PA binding under the experimental conditions employed. This behavior was not observed when the native sequence **15** was employed, demonstrating that the VME warhead is necessary for probe activity. Collectively, these findings establish that VME probe **19** is an effective ABP for selectively covalently targeting endogenous OTUB1 in complex environments.

CONCLUSION

In conclusion, we report the successful development of a novel strategy to perform ABPP of peptidic ABPs, bearing a VME warhead and a biotin tag, incorporated during solid phase peptide synthesis. This strategy was applied to covalent targeting of DUB enzyme OTUB1 with high selectivity at endogenous OTUB1 levels. The modular nature of this synthetic approach enabled the efficient and scalable assembly of diverse biotinylated probes, simplifying purification and downstream applications. Moreover, we report the synthesis of a novel VME-functionalized Fmoc-protected UAA that was shown to be compatible with SPPS. Biological evaluation demonstrated that four ABPs **16**−**17** and **18**−**19** effectively labeled recombinant OTUB1, even in the presence of thiol-containing protein BSA, suggesting a degree of selectivity for the catalytic cysteine of OTUB1. Notably VME probe **19** demonstrated robust labeling of native OTUB1 in HCT116 lysate, supporting its application as a reliable warhead for interrogating DUBs and cysteine isopeptidases in physiologically relevant systems. In contrast, propargyl-based probes did not exhibit detectable OTUB1 labeling in lysates, likely reflecting lower electrophilic reactivity under these conditions. These results highlight the critical importance of employing a diverse panel of electrophilic warheads when targeting cysteine isopeptidases such as OTUB1 or other DUBs, as different reactive groups can dramatically influence reactivity and selectivity in complex biological systems. Our approach, employing Fmoc-protected UAAs as interchangeable building blocks with diverse electrophilic warheads and peptide sequences enables the rapid assembly of peptidic probes in order to systematically survey reactivity and selectivity of cysteine isopeptidases such as OTUB1. These findings pave the way for future proteomic studies aimed at mapping OTUB1 activity and interactions in diverse cellular contexts with potential applications in biomarker discovery and therapeutic development targeting ubiquitin signaling pathways. In addition, the peptidic ABPs developed in this work are polar and enriched in positively charged residues, a feature associated with several cell-penetrating peptides that interact favorably with negatively charged membrane components. Such electrostatic interactions may support a degree of cellular uptake, although translocation efficiency is known to be sequence- and cell-type dependent.[27] Although this has not been examined in this study, the possibility of using ABP **19**

https://doi.org/10.1021/acschembio.5c00771
ACS Chem. Biol. XXXX, XXX, XXX−XXX

and its derivatives in live cell experiments is an exciting avenue for future studies. More broadly, the modular strategy described here can be adapted to target a wide range of cysteine-containing enzymes, providing a useful tool to enrich our current knowledge of a class of poorly understood, yet highly important, enzymes.

CHEMICAL METHODS

NMR spectra were recorded on an Agilent MR 400 spectrometer with operating frequencies of 399.84 MHz for ^{1}H and 100.55 MHz for ^{13}C, a Bruker Avance III 400 spectrometer with operating frequencies of 400.23 MHz for ^{1}H and 100.63 MHz for ^{13}C, or a Bruker Avance II 600 spectrometer with operating frequencies of 600.13 MHz for ^{1}H and 150.90 MHz for ^{13}C. NMR spectra were processed by using MestReNova. ^{1}H NMR chemical shifts were referenced to residual nondeuterated solvent peaks within the NMR solvent; $CHCl_3$ (d_H = 7.26 ppm) and DMSO (d_H = 2.50 ppm). The chemical shifts (δ) are reported in parts per million (ppm) and signal multiplicity as s = singlet, d = doublet, t = triplet, q = quartet, p = pentet, m = multiplet, and combinations thereof. Coupling constants (J) are quoted in Hertz (Hz) and reported to the nearest 0.1 Hz. ^{13}C NMR spectra are proton-decoupled with chemical shifts referenced to residual deuterated solvent peaks in the NMR solvent; $CDCl_3$ (d_C = 77.16 ppm) and DMSO-d_6 (d_C = 39.52 ppm). Product identification and peak assignments were carried out using additional 1D experiments (TOCSY), 2D experiments (HSQC, HMBC), and pulse experiments (DEPT-135) where appropriate. Mass spectrometry measurements were carried out on a Bruker ESI or APCI HRMS. Flash column chromatography was carried out using silica gel, particle size of 0.04−0.063 mm, purchased from Sigma-Aldrich or VWR. RT is classified in this work as 19.5−20.5 °C. TLC analysis was performed on TLC Silica gel 60 F_{254} plates purchased from Merck and visualized by UV irradiation (254 nm), potassium permanganate stain (3 g of $KMnO_4$, 20 g of K_2CO_3, 300 mL of H_2O), ammonium molybdate staining (0.26 M ammonium molybdate in 1 M aq. H_2SO_4), ninhydrin stain (1.5 g of ninhydrin, 5 mL of AcOH, 500 mL of 95% EtOH), and anisaldehyde stain (9.2 mL of *p*-methoxybenzaldehyde, 3.75 mL of AcOH, 338 mL of 95% EtOH, 12.5 mL of conc. H_2SO_4). All solvents were obtained from commercial sources and used as received. Anhydrous DCM, THF, Et_2O, and MeCN were obtained from a PureSolv solvent purification system, and DMF was used dry from SureSeal bottles. Petroleum ether refers to the fraction of petroleum ether that boils at 40−60 °C.

PEPTIDE SYNTHESIS GENERAL METHODS

General Procedure 1: First Amino Acid Coupling to Rink Amide Resin. Rink amide AM resin (0.78 mmol/g, 100−200 mesh, 1.0 equiv) was added to a SPPS syringe (Carl Roth GmbH, Karlsruhe, Germany) followed by DMF (4 mL). The syringe was agitated for 20 min and then drained. The resin was treated with 20% (v/v) piperidine in DMF (4 mL) for 2 × 10 min. The deprotected resin was then washed with DMF (3 × 5 mL), DCM (3 × 5 mL), and DMF (3 × 5 mL). PyBOP (4.0 equiv) and NMM (8.0 equiv) were added to a solution of Fmoc protected amino acid (4.0 equiv, 0.2 M) in DMF. This solution was transferred to the resin in the syringe and agitated for 45 min. Excess reagents were drained from the syringe, and the resin was washed with DMF (3 × 5 mL), DCM (3 × 5 mL), and DMF (3 × 5 mL).

General Procedure 2: Bromophenol Blue Monitoring of Coupling and Deprotection Reactions. The extent of each coupling reaction was qualitatively monitored by treatment of 5−10 resin beads with a solution of bromophenol blue (BPB) in DCM (0.15 mM, 0.1 mL). The following amino acid was coupled only when the beads turned blue upon treatment with BPB.

General Procedure 3: Second and Subsequent Amino Acid Fmoc Deprotection and Coupling. The following amino acid coupling cycles consisted of (I) Fmoc deprotection by the addition of 20% (v/v) piperidine in DMF (4 mL) to the resin for 2 × 10 min; (II) Resin washes with DMF (3 × 5 mL), DCM (3 × 5 mL), and DMF (3 × 5 mL); (III) Peptide coupling with addition of PyBOP (3.0 equiv), NMM (6.0 equiv), and N-protected amino acid (3.0 equiv, 0.2 M) in DMF to the peptide resin for 45 min; (IV) Resin washes with DMF (3 × 5 mL), DCM (3 × 5 mL), and DMF (3 × 5 mL); (V) Qualitative BPB test as per General Procedure 2. Following the final coupling, the resin was treated with 20% (v/v) piperidine in DMF (2 × 10 min, 5 mL), and the resin was washed with 2 rounds of DMF (3 × 5 mL) and DCM (3 × 5 mL), followed by drying of the resin under reduced pressure.

General Procedure 4: Resin Cleavage and Global Deprotection. DCM (4 mL) was added to dry peptide resin. The syringe was agitated for 20 min and then drained. The cleavage cocktail (TFA:TES:H_2O; 95:2.5:2.5 v/v/v; 5 mL) was transferred to the syringe, which was agitated for 90 min. The syringe was drained, and the filtrate was collected. The resin was washed with cleavage cocktail (2 × 3 mL), and the washings were combined with the first filtrate. The combined solution was concentrated under a flow of N_2 into a viscous oil, followed by precipitation of the crude peptide with Et_2O (7 mL). The peptide was washed with Et_2O (2 × 10 mL), and the crude solid was dried under reduced pressure.

General Procedure 5: On Resin Biotinylation. DMF (4 mL) was added to dry peptide resin. The syringe was agitated for 20 min and then drained. D-Biotin (146 mg, 0.6 mmol), PyBOP (312 mg, 0.6 mmol), and NMM (132 μL, 0.6 mmol) were dissolved in 4 mL of a 1:1 DMF:DMSO mixture. The coupling cocktail was transferred to the syringe, which was agitated at RT for 24 h. Following the final coupling, the resin was washed with 2 rounds of DMF (3 × 5 mL) and DCM (3 × 5 mL), followed by drying of the resin under reduced pressure.

BIOLOGICAL METHODS

Silver Staining. Gels were treated with a fixative solution at RT for 1 h or at 4 °C for 16 h. Gels were washed in 20% EtOH (2 × 10 min) and then in H_2O (2 × 10 min). Gels were sensitized in aq. $Na_2S_2O_3$ (0.02%) for 1 min and then immediately washed with H_2O (2 × 1 min). Gels were incubated in a solution of $AgNO_3$ (12 mM) with formaldehyde (0.02%) at 4 °C for a minimum of 20 min and for up to 2 h. Following this, gels were washed in H_2O (2 × 30 s) and transferred to the developer solution. Development was stopped using 5% AcOH. All gels were imaged using a Typhoon FLA9500 imager (GE Healthcare, Illinois USA).

Antibiotin Western Blot. A nitrocellulose membrane (GE Healthcare, Illinois USA) was soaked in blotting transfer buffer along with the filter papers and sponges that would form the transfer sandwich. The sandwich was assembled by starting from a black plate on top of which two wetted sponges and a filter paper were positioned. The acrylamide gel was transferred to the top of the filter paper, and the nitrocellulose membrane was placed on top of it, followed by filter paper, two sponges, and a red plate. Proteins were transferred onto the nitrocellulose membrane in blotting transfer buffer overnight at 15 V and 4 °C. The membrane was incubated in 20 mL of BSA blocking buffer (5% BSA in PBS-T) for 1 h at 4 °C with shaking at 140 rpm. The membrane was incubated in 12 mL of a BSA imaging solution (2.5% BSA in PBS-T, 0.1% SDS, 0.2 μg/mL of IRDye 800CW-Streptavidin) for 1 h at 4 °C with shaking at 140 rpm. The membrane was washed with PBS-T (4 × 5 min) prior to imaging. Biotinylated proteins were detected by near-infrared fluorescence (excitation 778 nm, emission 794 nm) on an Odyssey XF Infrared Imaging System (LI-COR Biosciences, Nebraska, USA).

Cell Lysis through Mechanical Methods. A cell pellet (100−200 μL) was combined with an equivalent amount of glass beads (500−750 μm, Acros Organics, New Jersey, USA) in an Eppendorf flask, and 200−400 μL of homogenization buffer was added. The Eppendorf was vortexed for 20 s and immediately cooled for 90 s on ice. Lysing and cooling steps were repeated 20 times. The resulting cell contents were centrifuged 13,200 rpm for 5 min. The supernatant was separated and stored on ice immediately. The supernatant was aliquoted into 10 μL aliquots for storage at −73 °C. Concentration was analyzed by a Nanodrop 1000 instrument (Protein A280).

https://doi.org/10.1021/acschembio.5c00771
ACS Chem. Biol. XXXX, XXX, XXX−XXX

Expression and Purification of OTUB1. The expression and purification of His tagged OTUB1 was carried out according to literature procedures.[13,28] BL21 (DE3) cells transfected with a pET28a-LIC vector containing an N-terminal His6 tagged OTUB1 were transferred from a glycerol stock into LB medium (8 mL) containing kanamycin (100 μg/mL) and grown for 18 h at 37 °C and 180 rpm. The cells were transferred into fresh LB medium (300 mL) containing kanamycin (100 μg/mL) and grown at 37 °C and 180 rpm until an OD_{600} of 0.6 to 0.9 was reached. IPTG was added at a final concentration of 0.4 mM, and the bacteria were incubated at 18 °C for 16 h with vigorous shaking. The cells were centrifuged at 6,000 rpm for 15 min. The resulting pellet was resuspended in homogenate buffer (25 mL) containing PMSF (20 μM) and lysed via sonication. The lysate was centrifuged at 13,000 rpm for 45 min. Ni NTA agarose resin (Sigma-Aldrich, Missouri, USA) (1.5 mL, 1:1 suspension in 20% EtOH) was centrifuged at 2,200 rpm for 5 min, and the supernatant was discarded. H2O (2 × 0.7 mL) was added to the beads, which were gently inverted until the resin was fully resuspended. The resulting solution was centrifuged at 2,200 rpm, and the supernatant was discarded. Ni wash buffer (1.4 mL) was added to the resin, which was transferred to the clarified supernatant and incubated overnight at 4 °C with rolling. The resin was centrifuged at 2,200 rpm, and the supernatant was discarded. Ni wash buffer (1 mL) was added to the resin, which was fully resuspended by gentle inversion and centrifuged at 2,200 rpm for 5 min. This wash step was repeated four times. The supernatant was discarded after each washing step. Ni elution buffer A (4 × 0.7 mL) was added to the resin that was resuspended by gentle inversion. The solution was centrifuged at 2,200 rpm for 5 min, and the supernatants from these washes were pooled in clean micro-centrifuge tubes. A final wash step was carried out with Ni elution buffer B (1 mL) at 2,200 rpm for 5 min. The supernatant was discarded, and the beads were stored in 20% EtOH. The pooled supernatants were concentrated in a 10 kDa MW cutoff Vivaspin 500 centrifugal concentrator in a centrifuge at 9,000 rpm to a final concentration of 50 μL. Ni wash buffer (450 μL) was added to the tubes and concentrated to 50 μL in a centrifuge at 9,000 rpm. This wash step was repeated, and the solution was resuspended in storage buffer (150 μL, 20 mM Tris-Cl pH 8.0, 1 mM DTT, 10% glycerol, 50 mM NaCl). The concentration was measured by nanodrop.

Activity-Based DUB Labeling in Cell Lysate Using HA-Ub-PA. HCT116 cells were seeded at 500,000 cells/mL overnight at 37 °C. The media were removed, and cells were washed with PBS prior to lysing in TRIS-lysis buffer (50 mM Tris, pH 7.5, 50 mM NaCl, 0.1% (v/v) NP-40, 0.5% (w/v) CHAPS, 2 mM $MgCl_2$, 5 mM BME, 10 U Benzonase, cOmplete EDTA-free protease inhibitor cocktail (Roche)). The probes were added to lysate (25 μg) at indicated concentrations and incubated for 1 h at 37 °C. HA-Ahx-Ahx-Ub-PA (0.5 μg, UbiQ Bio, catalog number: UbiQ-078) was added to lysate and incubated for 45 min at RT. 4× sample loading buffer containing 10% (v/v) β-mercaptoethanol was added, and samples were heated for 5 min at 95 °C. Proteins were separated by precast SDS-PAGE gel (4−15%, Bio-RAD) and transferred to nitrocellulose membranes (Amersham Protran, GE Healthcare) by Turbo transfer (Bio-RAD) in 1× Turbo transfer buffer supplemented with 20% (v/v) ethanol. Membranes were blocked in 5% (w/v) slimmed milk in Tris-buffer (50 mM Tris, pH 7.4, 150 mM NaCl) containing 0.01% (v/v) Tween-20 (TBST) for 1 h before incubation with the following primary antibody in the corresponding buffer overnight at 4 °C: OTUB1 (Cell signaling, 3783T): 1:1000 in 5% BSA in TBST; Vinculin (abcam, ab91459): 1:2000 in 5% BSA in TBST. The membrane was washed three times with 10 mL of TBST for 5 min and incubated with the corresponding fluorescent secondary antibody in 5% (w/v) BSA in TBST for 1 h at RT. After three washes with 10 mL of TBST (10 min each), the membrane was imaged with an Odyssey M imager.

■ ASSOCIATED CONTENT

Supporting Information

The Supporting Information is available free of charge at https://pubs.acs.org/doi/10.1021/acschembio.5c00771.

Additional experimental details including experimental methods, characterization data of novel compounds, silver-stained gel images, and full Western blot gel images (PDF)

■ AUTHOR INFORMATION

Corresponding Author

Joanna F. McGouran − *School of Chemistry, Trinity Biomedical Sciences Institute, Trinity College Dublin, Dublin 152-160, Ireland; Synthesis and Solid State Pharmaceutical Centre (SSPC), Bernal Institute, Limerick V94 T9PX, Ireland;* orcid.org/0000-0002-9349-2141; Email: jmcgoura@tcd.ie

Authors

Valerio Cataldi − *School of Chemistry, Trinity Biomedical Sciences Institute, Trinity College Dublin, Dublin 152-160, Ireland*

Nikita Ostrovitsa − *School of Chemistry, Trinity Biomedical Sciences Institute, Trinity College Dublin, Dublin 152-160, Ireland*

Fangyuan Cao − *Molecular Sciences Research Hub, Imperial College London, London W12 0BZ, United Kingdom*

Edward W. Tate − *Molecular Sciences Research Hub, Imperial College London, London W12 0BZ, United Kingdom;* orcid.org/0000-0003-2213-5814

Eoin M. Scanlan − *School of Chemistry, Trinity Biomedical Sciences Institute, Trinity College Dublin, Dublin 152-160, Ireland*

Complete contact information is available at: https://pubs.acs.org/10.1021/acschembio.5c00771

Notes

The authors declare no competing financial interest.

■ ACKNOWLEDGMENTS

This publication was supported by the Irish Research Council (IRC) postgraduate scholarship Grant No. GOIPG/2020/1088.

■ REFERENCES

(1) Damgaard, R. B. The ubiquitin system: from cell signalling to disease biology and new therapeutic opportunities. *Cell Death Differ.* **2021**, *28* (2), 423−426.

(2) Clague, M. J.; Urbe, S.; Komander, D. Breaking the chains: deubiquitylating enzyme specificity begets function. *Nat. Rev. Mol. Cell Biol.* **2019**, *20* (6), 338−352.

(3) Dewson, G.; Eichhorn, P. J. A.; Komander, D. Deubiquitinases in cancer. *Nat. Rev. Cancer* **2023**, *23* (12), 842−862.

(4) Li, S.; Zhao, J.; Shang, D.; Kass, D. J.; Zhao, Y. Ubiquitination and deubiquitination emerge as players in idiopathic pulmonary fibrosis pathogenesis and treatment. *JCI Insight* **2018**, *3* (10), e120362.

(5) Parihar, N.; Bhatt, L. K. Deubiquitylating enzymes: potential target in autoimmune diseases. *Inflammopharmacology* **2021**, *29* (6), 1683−1699.

(6) Wiener, R.; Zhang, X.; Wang, T.; Wolberger, C. The mechanism of OTUB1-mediated inhibition of ubiquitination. *Nature* **2012**, *483* (7391), 618−622.

(7) Edelmann, M. J.; Iphofer, A.; Akutsu, M.; Altun, M.; di Gleria, K.; Kramer, H. B.; Fiebiger, E.; Dhe-Paganon, S.; Kessler, B. M. Structural basis and specificity of human otubain 1-mediated deubiquitination. *Biochem. J.* **2009**, *418* (2), 379−390.
(8) Saldana, M.; VanderVorst, K.; Berg, A. L.; Lee, H.; Carraway, K. L. Otubain 1: a non-canonical deubiquitinase with an emerging role in cancer. *Endocr Relat Cancer* **2019**, *26* (1), R1−R14.
(9) Liao, Y.; Yang, M.; Wang, K.; Wang, Y.; Zhong, B.; Jiang, N. Deubiquitinating enzyme OTUB1 in immunity and cancer: Good player or bad actor? *Cancer Lett.* **2022**, *526*, 248−258.
(10) Wu, M.; Sun, L.; Song, T. OTUB1-mediated inhibition of ubiquitination: a growing list of effectors, multiplex mechanisms, and versatile functions. *Front Mol. Biosci* **2024**, *10*, 1261273.
(11) Borodovsky, A.; Kessler, B. M.; Casagrande, R.; Overkleeft, H. S.; Wilkinson, K. D.; Ploegh, H. L. A novel active site-directed probe specific for deubiquitylating enzymes reveals proteasome association of USP14. *EMBO J.* **2001**, *20* (18), 5187−5196.
(12) Verhelst, S. H. L.; Bonger, K. M.; Willems, L. I. Bioorthogonal Reactions in Activity-Based Protein Profiling. *Molecules* **2020**, *25* (24), 5994.
(13) Borodovsky, A.; Ovaa, H.; Kolli, N.; Gan-Erdene, T.; Wilkinson, K. D.; Ploegh, H. L.; Kessler, B. M. Chemistry-based functional proteomics reveals novel members of the deubiquitinating enzyme family. *Chem. Biol.* **2002**, *9* (10), 1149−1159.
(14) Love, K. R.; Pandya, R. K.; Spooner, E.; Ploegh, H. L. Ubiquitin C-terminal electrophiles are activity-based probes for identification and mechanistic study of ubiquitin conjugating machinery. *ACS Chem. Biol.* **2009**, *4* (4), 275−287.
(15) Ekkebus, R.; van Kasteren, S. I.; Kulathu, Y.; Scholten, A.; Berlin, I.; Geurink, P. P.; de Jong, A.; Goerdayal, S.; Neefjes, J.; Heck, A. J.; et al. On terminal alkynes that can react with active-site cysteine nucleophiles in proteases. *J. Am. Chem. Soc.* **2013**, *135* (8), 2867−2870.
(16) de Jong, A.; Witting, K.; Kooij, R.; Flierman, D.; Ovaa, H. Release of Enzymatically Active Deubiquitinating Enzymes upon Reversible Capture by Disulfide Ubiquitin Reagents. *Angew. Chem., Int. Ed. Engl.* **2017**, *56* (42), 12967−12970.
(17) McGouran, J. F.; Gaertner, S. R.; Altun, M.; Kramer, H. B.; Kessler, B. M. Deubiquitinating enzyme specificity for ubiquitin chain topology profiled by di-ubiquitin activity probes. *Chem. Biol.* **2013**, *20* (12), 1447−1455.
(18) Taylor, N. C.; Hessman, G.; Kramer, H. B.; McGouran, J. F. Probing enzymatic activity - a radical approach. *Chem. Sci.* **2020**, *11* (11), 2967−2972.
(19) Taylor, N. C.; McGouran, J. F. Strategies to Target Specific Components of the Ubiquitin Conjugation/Deconjugation Machinery. *Front Chem.* **2020**, *7*, 914.
(20) El Oualid, F.; Merkx, R.; Ekkebus, R.; Hameed, D. S.; Smit, J. J.; de Jong, A.; Hilkmann, H.; Sixma, T. K.; Ovaa, H. Chemical synthesis of ubiquitin, ubiquitin-based probes, and diubiquitin. *Angew. Chem., Int. Ed. Engl.* **2010**, *49* (52), 10149−10153.
(21) Sommer, S.; Weikart, N. D.; Linne, U.; Mootz, H. D. Covalent inhibition of SUMO and ubiquitin-specific cysteine proteases by an in situ thiol-alkyne addition. *Bioorg. Med. Chem.* **2013**, *21* (9), 2511−2517.
(22) Albrow, V. E.; Ponder, E. L.; Fasci, D.; Bekes, M.; Deu, E.; Salvesen, G. S.; Bogyo, M. Development of small molecule inhibitors and probes of human SUMO deconjugating proteases. *Chem. Biol.* **2011**, *18* (6), 722−732.
(23) Ngo, C.; Fried, W.; Aliyari, S.; Feng, J.; Qin, C.; Zhang, S.; Yang, H.; Shanaa, J.; Feng, P.; Cheng, G.; et al. Alkyne as a Latent Warhead to Covalently Target SARS-CoV-2 Main Protease. *J. Med. Chem.* **2023**, *66* (17), 12237−12248.
(24) Majorek, K. A.; Porebski, P. J.; Dayal, A.; Zimmerman, M. D.; Jablonska, K.; Stewart, A. J.; Chruszcz, M.; Minor, W. Structural and immunologic characterization of bovine, horse, and rabbit serum albumins. *Mol. Immunol* **2012**, *52* (3−4), 174−182.
(25) Ye, D.; Wang, S.; Wang, X.; Lin, Y.; Huang, Y.; Chi, P. Overexpression of OTU domain-containing ubiquitin aldehyde-binding protein 1 exacerbates colorectal cancer malignancy by inhibiting protein degradation of beta-Catenin via Ubiquitin-proteasome pathway. *Bioengineered* **2022**, *13* (4), 9106−9116.
(26) Niers, J. M.; Chen, J. W.; Weissleder, R.; Tannous, B. A. Enhanced in vivo imaging of metabolically biotinylated cell surface reporters. *Anal. Chem.* **2011**, *83* (3), 994−999.
(27) Yang, N. J.; Hinner, M. J. Getting across the cell membrane: an overview for small molecules, peptides, and proteins. *Methods Mol. Biol.* **2015**, *1266*, 29−53.
(28) Chong, S.; Mersha, F. B.; Comb, D. G.; Scott, M. E.; Landry, D.; Vence, L. M.; Perler, F. B.; Benner, J.; Kucera, R. B.; Hirvonen, C. A.; et al. Single-column purification of free recombinant proteins using a self-cleavable affinity tag derived from a protein splicing element. *Gene* **1997**, *192* (2), 271−281.

https://doi.org/10.1021/acschembio.5c00771
ACS Chem. Biol. XXXX, XXX, XXX−XXX